Physical characterization of high methoxyl pectin and sunflower oil wax emulsions: A low-field ^{1}H NMR relaxometry study

Sinem Akkaya, Baris Ozel, Mecit Halil Oztop, Derya Kocak Yanik, and Fahrettin Gogus

Abstract: Pectin–wax-based emulsion systems could be used to form edible films and coatings with desired water permeability characteristics. Pectin is often used in food industry due to its gelling and viscosity increasing properties. Physical properties of pectin are highly dependent on its esterification degree. Waxes are commonly used as edible coatings to enhance the water barrier properties of food products. This study focuses on preparing emulsions with sunflower oil wax (SFW) and high methoxyl pectin (HMP) at different concentrations for any possible edible film or coating formulations. Sunflower oil (SFO) was added as the dispersed oil phase to these emulsions. Characterization of the emulsions was performed by using particle size, rheology, and time domain nuclear magnetic resonance (NMR) relaxometry measurements. Effects of HMP concentration and the presence of SFO in the emulsion formulations were explored. Mean particle size values were recorded between 1 and 3 μm. Rheology measurements showed that increasing HMP concentrations and presence of SFO in emulsions resulted in more pseudoplastic behavior. NMR transverse relaxation times (T_2) were measured to detect the differences between the emulsions. Relaxation spectrum analysis was also conducted for a detailed understanding of the transverse relaxations. Addition of SFO and higher HMP concentrations decreased the T_2 values of the emulsion systems ($P < 0.05$). However, T_2 decreasing effect of SFO was compensated at 10% (w/w) HMP concentration showing that SFO was well dispersed in this particular emulsion formulation. Changes in the rheological behavior and relaxation times provided insight on the formation and stability of the emulsions.

Keywords: emulsions, pectin, TD-NMR relaxometry, wax

Practical Application: Findings of this study can be utilized and integrated to produce edible films and coatings with different water permeability characteristics. This study showed that NMR relaxometry parameters were also effective in monitoring and determining the physical characteristics of the pectin–wax-based emulsion systems as other conventional techniques including rheology and particle size measurements. Our NMR relaxometry findings were in correlation with the flow behavior and particle size results of the investigated emulsion systems.

1. INTRODUCTION

Oil-in-water (o/w) emulsions are the most encountered emulsions in food industry (Karbstein & Schubert, 1995). These emulsions need a third component for dispersion. This can be achieved by using some natural or synthetic materials, which are called emulsifiers or surfactants (Guzey & McClements, 2006). Emulsifiers are surface-active ingredients and they adsorb onto the surface of the lipid droplets during homogenization (Moreau, Kim, Decker, & McClements, 2003). Proteins are natural emulsifiers and they are generally used for such purposes (Dickinson, 2003). Hydrocolloids are also gaining interest as emulsifying agents in emulsion systems. In contrast to proteins and surfactants having hydrophobic parts, most hydrocolloids are hydrophilic polymers and they do not possess strong surface active properties. Due to these characteristics, hydrocolloids are usually considered as stabilizers (Dickinson, 2009). Prevention of oil droplets from aggregation and coalescence could be maintained by steric and electrostatic mechanisms in polysaccharide containing systems (Derkach, 2009; Ushikubo & Cunha, 2014). Polysaccharides are able to form a higher thickness of thin films between oil droplets with respect to proteins and surfactants (Chanamai & McClements, 2002). In this way, polysaccharides are able to modify the viscosity of aqueous continuous phase of the medium so that they can provide long-term stabilization (Taherian, Fustier, Britten, & Ramaswamy, 2008).

Strong hydrophilic character of polysaccharides reduces their surface active properties with respect to surfactants and proteins (Dickinson, 2009). However, presence of a small protein moiety, for example gum arabic or hydrophobic groups, for example methylated groups of high methoxyl pectin (HMP), can provide polysaccharides some emulsifier abilities (Huang, Kakuda, & Cui, 2001). For instance, pectin is a strongly hydrophilic polymer but the degree of esterification and polymerization determines the functional characteristics of pectin in aqueous solutions (Akhtar, Dickinson, Mazoyer, & Langendorff, 2002). Pectin provides stable emulsions mainly by electrostatic repulsion mechanism (Muhiddinov, Khalikov, Speaker, & Fassihi, 2004). High hydrophilic capacity of pectin limits its use in emulsion formulations designed for production of edible films and coatings with desirable water permeable characteristics. Nevertheless, combination of pectin with

JFDS-2020-1503 Submitted 8/25/2020, Accepted 11/18/2020. *Authors Akkaya, Yanik, and Gogus are with Food Engineering Department, Gaziantep University, Gaziantep, Turkey. Authors Akkaya, Ozel, and Oztop are with Food Engineering Department, Middle East Technical University, Ankara, Turkey. Author Ozel is with Food Engineering Department, Ahi Evran University, Kirsehir, Turkey. Direct inquiries to author Oztop (E-mail: mecit@metu.edu.tr).*

doi: 10.1111/1750-3841.15560

Journal of Food Science A Publication of the Institute of Food Technologists

Table 1–Composition of samples (w/w, %).

Sample	High methoxyl pectin (%)	Sunflower oil wax (%)	Sunflower oil (%)
S1	5	5	–
S2	7	5	–
S3	10	5	–
S4	5	5	10
S5	7	5	10
S6	10	5	10
S7	–	–	100
S8	5	–	–
S9	7	–	–
S10	10	–	–
S11	5	–	10
S12	7	–	10
S13	10	–	10
S14	–	33	67
S15	–	100	–

lipids can be used to form stable emulsions (Thakur, Singh, & Handa, 1997). Wax–pectin binary systems are suitable examples for such systems (Galus & Kadzińska, 2015; Vargas, Pastor, Chiralt, McClements, & González-Martínez, 2008). Waxes are lipid structures found in fruits and seeds with strong hydrophobic properties (Lee, 1999). Water impermeable properties of wax containing edible films are widely utilized in the food industry (Aguirre-Joya et al., 2019; Kowalczyk, Zięba, Skrzypek, & Baraniak, 2017; Zhang, Simpson, & Dumont, 2018). Sunflower oil wax (SFW) is among the wax sources, for example candeilla, beeswax used for such purposes. Additionally, SFW contains trace amount of crude oil giving the wax a bit of an amphiphilic character (Baümler, Carelli, & Martini, 2013).

In this study, HMP–SFW-based emulsions, both in the presence and absence of SFO, were formulated and characterized by particle size, rheology, and LF ^{1}H NMR experiments. Low methoxyl pectin (LMP) was mostly used in the previous pectin–SFW emulsion studies (Chalapud, Baümler, & Carelli, 2018, 2020). Accordingly, the primary objectives of this study were to show that HMP could also be used in wax containing edible film emulsion formulations and NMR relaxometry parameters could be correlated with the rheological and particle size characterizations. To the best of our knowledge, there is no NMR relaxometry study for the characterization of such emulsion systems in the literature.

2. MATERIALS AND METHODS

2.1 Materials

Medium rapid setting purified HMP (APA 103; Yantai Andre Pectin Co Ltd., Yantai, China) extracted from apple pomace with an esterification degree of 66 to 69%, SFW (Koster Keunen, Bladel, the Netherlands) with melting point around 74 to 77 °C, which was determined by preliminary differential scanning calorimetry (DSC) measurements and SFO (Yudum, Savola Foods, Istanbul, Turkey) were used as the main materials. Sodium azide (Merck KgaA, Darmstadt, Germany) was added to all emulsions at 0.1% (w/w) concentration to prevent microbial growth. All emulsions were prepared using distilled water.

2.2 Emulsion preparation

HMP solutions and SFW dispersions were prepared, separately. They were stirred separately at 300 rpm for 30 min at 80 °C. Since the melting point of SFW was around 75 °C, all samples were mixed at 80 °C to prevent wax crystallization. After SFW melted completely, HMP and SFW solutions were mixed with a high shear homogenizer (IKA; T18 Digital Ultra-Turrax) at 25,000 rpm for 5 min. Sodium azide was added into the emulsions (0.1%, w/w). Emulsions were cooled to room temperature after homogenization (~25 °C). For the SFO containing samples, SFO at 10% (w/w) concentration was added into the previously prepared HMP–SFW mixtures and homogenized again at 25,000 rpm for 5 min. HMP concentrations used in the study were determined by preliminary experiments to obtain stable emulsions. Compositions of the samples were given in Table 1.

2.3 Particle size measurements

Mean particle size values of the emulsions were determined by using a light diffraction based particle size analyzer (Mastersizer 3000 Malvern, Worcestershire, UK) and refractive index value of 1.56 was used (Guner & Oztop, 2017). Sample particles were assumed to be spherical and particle analyzer speed was adjusted to 2,000 rpm during the analyses. Each emulsion was brought to room temperature and diluted in deionized water prior to particle size analysis. Particle size values were described by the volume-based $D_{[4,3]}$ mean diameter as shown in Equation (1):

$$D_{[4,3]} = \Sigma N_i D_i^4 / N_i D_i^3 \quad (1)$$

where D_i value is the geometric mean of diameters, N_i is the number of particles in emulsion with diameter D_i.

2.4 Rheological measurements

Rheological characterization of the emulsions was performed by using a dynamic rheometer (Kinexus Dynamic Rheometer, Malvern, UK) with a cone-and-plate (40 mm diameter and 4° cone angle, 0.1425 mm gap) geometry. Emulsions at the room temperature were poured onto the plate so that the surface of the cone was fully covered with the sample. Then, shear stress values were recorded with varying shear rate values between 0.1 and 95 s^{-1}, in a total ramp time of 2 min (Thombre & Gide, 2013). Data were analyzed by Power Law, Newtonian, and Herschel–Bulkley models. The best fitted model was the Power Law model with the following equation (Eq. 2):

$$\tau = k\gamma^n \quad (2)$$

where τ, k, γ, and n denote shear stress, consistency index, shear rate, and flow behavior index, respectively.

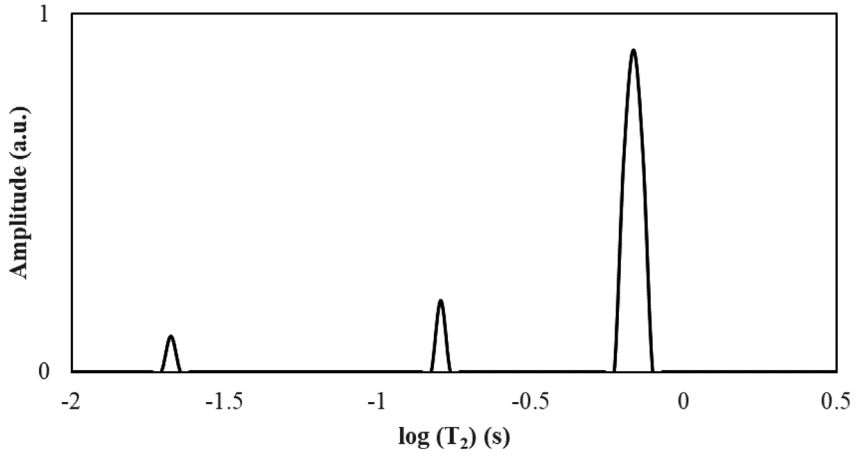

Figure 1–Representative transverse relaxation spectrum of the emulsions.

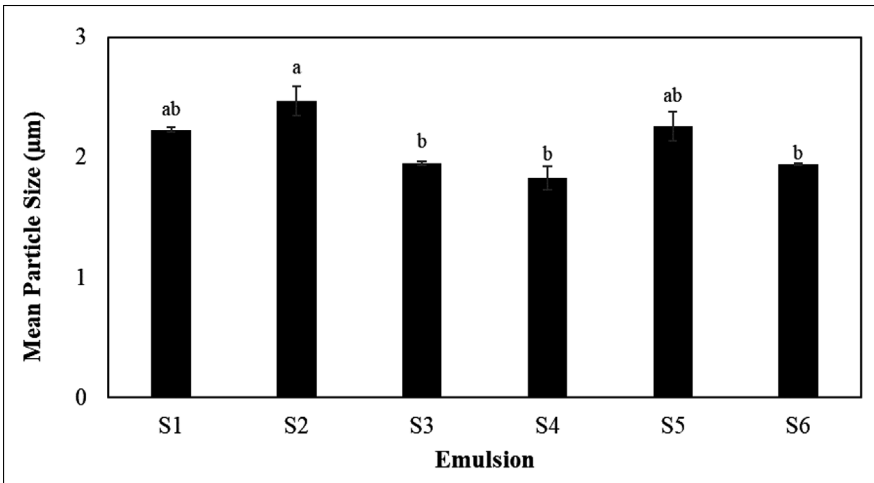

Figure 2–Mean particle size [D (4,3)] values of the emulsions.

2.5 NMR relaxometry measurements

2.5.1 Transverse relaxation measurements. NMR transverse relaxation times (T_2) of all emulsions were measured according to the method of Pocan, Ilhan, and Oztop (2019) using a LF NMR system equipped with a permanent magnet operating at a ^{1}H frequency of 22.40 MHz (Spin Core, Gainesville, FL, USA), having a 10 mm diameter radio frequency (RF) coil (Pocan et al., 2019). Prepared emulsions were allowed to equilibrate to room temperature and then poured into cylindrical tubes having 10 mm diameter for the measurements. Carr–Purcell–Meiboom–Gill (CPMG) sequence was used to measure the T_2 values. CPMG experiments were performed using a repetition delay of 3 s, echo time of 2,000 ms, 32 scans, and number of echoes changing between 1,500 and 3,000 depending on the sample. Decay curves were fitted to a mono-exponential fitting using MATLAB.

2.5.2 Relaxation spectrum analysis. In order to analyze the relaxation behaviors of the emulsions in detail, multiexponential decay fitting of the CPMG curves was implemented. For that purpose, Prospa 3.1 (Magritek, PA, USA) software was used. Non-negative-least-squares analysis which utilizes an Inverse Laplace based routine to decompose an exponential decaying curve to its multiexponential components was performed (Oztop, Rosenberg, Rosenberg, McCarthy, & McCarthy, 2010). Figure 1 shows a representative transverse relaxation spectrum of the emulsions.

2.6 Statistical analysis

Analysis of variance was used to analyze the experimental results with Minitab (Version 16.2.0.0; Minitab Inc., Coventry, UK). Tukey's comparison test at 95% confidence level was applied for the comparisons. Measurements were conducted as three independent replicates.

3. RESULTS AND DISCUSSION

3.1 Particle size analysis

Size and distribution of oil droplets determine the stability of an o/w emulsion (McClements, 2015). Mean particle size values of the S_1 to S_6 samples were in the range of 1.5 to 2.5 μm. Similar to our particle size results, it was previously stated that the average particle size of o/w canola emulsions stabilized with pectin was around 2.5 μm (Huang et al., 2001). As shown in Figure 2, average particle size of initial HMP–SFW dispersions (S_1) decreased when HMP concentration reached 10% (w/w; S_3; $P < 0.05$). However, higher HMP concentrations in SFO containing HMP–SFW emulsions did not change the mean particle size values of the emulsions (Figure 2). This could be attributed to the polydispersity values of the emulsions (Table 2) (McClements, 2015). Polydispersity results suggested that emulsions formed were not monomodel systems. Nakauma et al. (2008) stated that o/w emulsions having

Table 2–Particle polydispersity values of the emulsions.[a].

Sample	Mean particle span
S_1	2.31 ± 0.05^{a}
S_2	2.42 ± 0.25^{a}
S_3	1.42 ± 0.05^{b}
S_4	2.28 ± 0.80^{a}
S_5	2.78 ± 0.25^{a}
S_6	1.43 ± 0.02^{b}

[a]Different inline letters in each column indicate significant difference ($P < 0.05$). Errors are represented as standard deviations.

Table 3–Power Law constants of the emulsions.[a].

Sample	k (Pa·s^n)	n
S_1	0.26 ± 0.11^{d}	0.96 ± 0.02^{ab}
S_2	0.48 ± 0.07^{d}	0.96 ± 0.01^{a}
S_3	9.41 ± 0.13^{b}	0.86 ± 0.00^{d}
S_4	1.11 ± 0.27^{d}	0.92 ± 0.01^{bc}
S_5	4.54 ± 0.45^{c}	0.90 ± 0.01^{c}
S_6	20.97 ± 1.54^{a}	0.82 ± 0.01^{d}

[a]Different inline letters in each column indicate significant difference ($P < 0.05$). Errors are represented as standard deviations.

high emulsifier-to-oil ratio contained nonflocculated and polydisperse oil droplets (Nakauma et al., 2008). Under these conditions, HMP was able to reduce the mean particle size in SFW emulsions but it was not very effective on mean droplet size in SFW–SFO emulsions. Hydrodynamic processes which were induced by droplet disruption during homogenization may have controlled the mean droplet size values (Jafari, Assadpoor, He, & Bhandari, 2008). Nakauma et al. (2008) also showed that o/w emulsions containing sugar beet pectin, soybean soluble polysaccharide, and gum arabic emulsifiers had stable droplet size distributions after a critical emulsifier-to-oil ratio. These emulsions experienced substantial increase in their continuous phase viscosities which induced constant average droplet size values starting from emulsifier-to-oil ratios of 0.14, 0.34, and 0.67 for sugar beet pectin, soybean soluble polysaccharide, and gum arabic, respectively (Nakauma et al., 2008). In our study, high emulsifier/oil ratios of 0.5, 0.7, and 1.0 were used. Therefore, even at 10% (w/w) HMP, similar droplet size distributions were observed in SFO containing samples (S_4 to S_6).

Besides mean particle size results, polydispersity analysis of the emulsion systems can also provide valuable information on the emulsion quality and characteristics (Riquelme, Zúñiga, & Arancibia, 2019). SFO emulsions containing candeilla and carnauba waxes had higher polydispersity values with respect to the emulsion prepared with stearic acid, according to a study which investigated solid lipid dispersions (Asumadu-Mensah, Smith, & Ribeiro, 2013). Similarly, we have also observed higher mean particle span values for the SFW containing samples than expected except for the samples with 10% (w/w) HMP. Table 2 demonstrated that S_3 and S_6 formulations had lower span values with respect to other formulations ($P < 0.05$). Span results suggested that HMP could produce more similar sized oil droplets at 10% (w/w) concentration. Chalapud et al. (2018) demonstrated that LMP (1 to 3%, w/w) was able to produce SFW emulsions with mean particle size and polydispersity values in the range of 4.80 to 8.60 μm and 1.10 to 2.04, respectively (Chalapud et al., 2018). When compared to this study, our results suggested that HMP could produce smaller mean particle size values for the emulsions at all HMP concentrations (Figure 2). However, 10% (w/w) HMP was required to attain low span values as reported for LMP stabilized SFW emulsions (Table 2). In general, effective emulsifiers rapidly reduce oil–water interfacial tension, adsorb strongly onto the oil droplets and prevent recoalescence of droplets via electrostatic and steric repulsion mechanisms (Leroux, Langendorff, Schick, Vaishnav, & Mazoyer, 2003). In case of hydrophilic hydrocolloids such as pectin and its derivatives, required amount to saturate the droplet surface is higher than the small emulsifier particles (Dickinson, 2009). Thus, a high HMP concentration around 10% (w/w) was needed to observe the stabilizing effect of HMP. Despite its weak surface activity properties, HMP may have exhibited some interfacial activity via slow migration to the oil–water interphase at high concentrations (Garti & Reichman, 1993). When surfaces of oil droplets are not completely covered, a single polymer chain can interact with many particles and cause bridging flocculation of some droplets (Dickinson, 2009). This was probably the case in S_5 samples since at 7% (w/w) HMP concentration, emulsion droplets had similar droplet sizes and higher span values with respect to S_6 samples. Below droplet surface saturation coverage, emulsions could not maintain stable profiles. At 10% (w/w) HMP concentration (S_6), oil droplets were probably fully covered with the polymer and these coated droplets repelled each other due to anionic character of HMP.

Another factor which affected the size and distribution of the particles was the presence of SFW in the emulsion system. The lower mean particle size and reduction in polydispersity values of S_3 showed that HMP surrounded molten wax droplets during homogenization at 10% (w/w) concentration (Leroux et al., 2003). Shortly after homogenization, molten wax particles started solidifying and then they crystallized. Clearly, at 10% (w/w) HMP, nucleation and growth of wax crystals were hindered. By this way, presence of SFW also contributed to the higher stability of SFO containing emulsions at 10% HMP concentration (S_6).

3.2 Rheological analysis

Rheological behaviors of the emulsions were evaluated and composition of emulsions were found to be effective on the flow behaviors (Kim & Mason, 2017). All samples had shear-thinning characteristics as shown in Figure 3(A, B). First, increasing HMP concentration resulted in higher consistency index values, thus higher resistance to flow (Table 3; $P < 0.05$; Sahin & Sumnu, 2006). Viscosity increase was more predominant in SFO containing samples. Flow behavior index values decreased with increasing HMP concentration and emulsions obtained a more shear-thinning character ($P < 0.05$; Sahin & Sumnu, 2006). Presence of SFO enhanced the pseudoplastic character of the samples. Although S_6 had considerably higher consistency index than S_3, their flow behavior index values were statistically same indicating that SFO was successfully incorporated into the HMP–SFW system of S_6 ($P > 0.05$; Tabilo-Munizaga & Barbosa-Cánovas, 2005).

Predominantly hydrophilic, high molecular weight (10^4 to 10^6 Da) polymers may form a thick steric stabilizing layer between oil droplets (Pal, 1996). Furthermore, polymers having charged groups in their structures may establish net electrostatic repulsive forces between the oil droplets (Guzey & McClements, 2006). HMP is an anionic, high molecular weight (~840 kDa) polymer that is suitable for the aforementioned stabilizing mechanisms (Ushikubo & Cunha, 2014). Before forming a thick layer between the oil droplets, HMP may have produced a charged stabilizing layer via its ionizable groups in the system at 5% (w/w) concentration. Substantial increments in viscosities of the samples were observed (Table 3) starting from HMP concentrations of 7% (w/w)

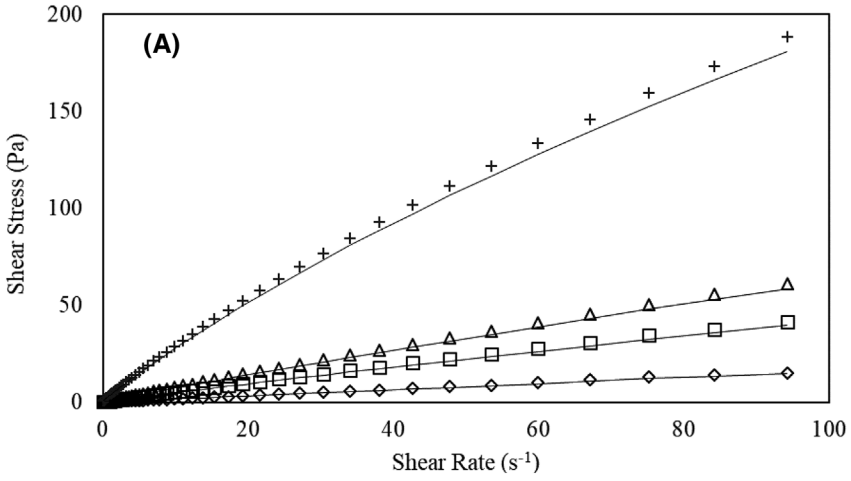

Figure 3A–Flow behavior curves of ◊, S_1; □, S_2; Δ, S_4; +, S_5.

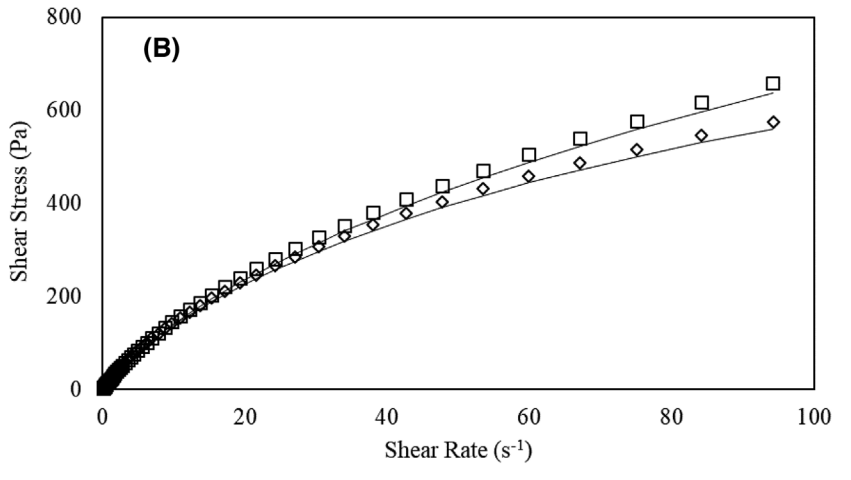

Figure 3B–Flow behavior curves of ◊, S_3; □, S_6.

and especially at 10% (w/w). Therefore, thickness of the layers between oil droplets may have been enhanced extensively so that this mechanism may have predominated the emulsion system (Dickinson, 2009). Increase in the polymer (HMP) concentration might have also contributed to the viscosity increase to some extent but it is highly unlikely that amount of HMP can alone induce such a dramatic change in the flow behaviors of the samples. Probably, HMP was able to increase the viscosity of the continuous phase surrounding the oil droplets since the emulsifier concentration was high. In this way, mobility of the oil droplets was restricted (Chanamai & McClements, 2002). Okuro, Gomes, Costa, Adame, and Cunha (2019) also claimed that increasing emulsifier (lecithin) content in o/w emulsions with 25% (w/w) SFO formed an enhanced viscoelastic interfacial layer which provided a good kinetic stability to their emulsions (Okuro et al., 2019). In another study, pea protein–polysaccharide complexes prepared with different polysaccharides were used to stabilize the SFO containing o/w emulsions at 2% (w/w) total polymer concentration (Vélez-Erazo, Bosqui, Rabelo, Kurozawa, & Hubinger, 2020). They showed that pea protein–tara gum and pea protein– xanthan gum complexes provided a better stability to the emulsions since xanthan gum and tara gum produced more viscous samples. In spite of the fact that pea protein–gum arabic and pea protein–pectin containing emulsions also demonstrated some pseudoplastic behavior, viscosities of these emulsions were lower than the ones with xanthan gum and tara gum. Consequently, pectin and gum arabic including emulsions did not exert a good stability over time (Vélez-Erazo et al., 2020). In this sense, a high HMP concentration (10%, w/w) was required in our study to obtain stable emulsions with more viscous character. Additionally, viscosity and storage moduli of fine emulsions were reported to be higher than that of coarse emulsions and for the fine emulsions the shear-thinning effect was much stronger (Barnes, 1994). Therefore, increase in the bulk viscosity and enhanced pseudoplastic behavior of emulsions were attributed to better stability (Pal, 1996). After acquiring more viscoelastic character, emulsions were less prone to bridging flocculation (Xiong et al., 2018). Lower span value of S_6 with respect to S_4 and S_5 samples was also in agreement with these findings ($P < 0.05$). Now, NMR relaxometry results will be discussed in detail to investigate any possible correlation with the particle size and rheological characterization of the emulsions.

3.3 NMR relaxometry analysis

3.3.1 Mono-exponential transverse relaxation times. Mono-exponential transverse relaxation times of emulsions were analyzed to investigate the effects of ingredients and compositions of the emulsions. As will be seen in Section 3.3.2, multicompartmental relaxation analysis of the samples was also

Table 4–Mono-exponential transverse relaxation times of the emulsions (S_1 to S_6) and high methoxyl pectin solutions (S_8 to S_{10}).[a] .

Sample	T_2 (ms)
S_1	312.48 ± 4.70^{b}
S_2	197.62 ± 1.26^{e}
S_3	115.24 ± 1.87^{h}
S_4	268.06 ± 8.35^{c}
S_5	174.64 ± 8.49^{f}
S_6	111.73 ± 0.85^{h}
S_8	347.77 ± 5.59^{a}
S_9	240.81 ± 3.76^{d}
S_{10}	141.14 ± 1.47^{g}

[a]Different inline letters in each column indicate significant difference ($P < 0.05$). Errors are represented as standard deviations.

Table 5–Mono-exponential transverse relaxation times of the emulsions (S_4 to S_6) and (S_{11} to S_{13}).

Sample	T_2 (ms)
S_4	268.06 ± 8.35^{b}
S_5	174.64 ± 8.49^{d}
S_6	111.73 ± 0.85^{e}
S_{11}	380.23 ± 11.66^{a}
S_{12}	212.94 ± 2.14^{c}
S_{13}	133.41 ± 0.63^{de}

[a]Different inline letters in each column indicate significant difference ($P < 0.05$). Errors are represented as standard deviations.

performed for a more detailed discussion. Table 4 summarizes the mono-exponential T_2 results of the emulsions. Applied RF pulse generates a signal representing the whole sample. Therefore, it is crucial to distinguish the information obtained during the relaxation process (Hashemi, Bradley, & Lisanti, 2010). T_2 is related to the efficiency of the energy transfer between neighboring spins (Kirtil & Oztop, 2016). If the molecules of a sample have short distances between each other, a high energy transfer efficiency is achieved producing shorter T_2. Thus, solid materials having closely packed molecules have shorter T_2 than liquid materials such as water whose molecules have larger distances between each other (Hashemi et al., 2010). Long T_2 of water predominates the transverse relaxation characteristics of the food materials with high water content, for example o/w emulsions. Therefore, the mono-exponential T_2 of an o/w emulsion is mostly affected by the mobility and distribution of water protons within the emulsion system (Linke, Guthausen, Flöter, & Drusch, 2018). First, a continuous reduction in T_2 of HMP–SFW containing samples (S_1 to S_3) was observed with higher HMP concentrations ($P < 0.05$). Same trend of T_2 was also applicable for the SFO added samples (S_4 to S_6). In general, SFO containing samples maintained a lower T_2 profile compared to their no SFO containing correspondents ($P < 0.05$). However, T_2 of S_3 and S_6 were similar indicating that T_2 decreasing effect of SFO was compensated at 10% (w/w) HMP. T_2 is also known as spin–spin relaxation time and measures the ^{1}H proton relaxation rates in the transverse plane (Hashemi et al., 2010). In this study, emulsions contained at least 85% (w/w) water thus, the information provided by T_2 could be used to evaluate the state of water interacting with the surrounding macromolecules (Williams, Oztop, Mccarthy, Mccarthy, & Lo, 2011). Water in free state with a flexible molecular packing, attains longer T_2 (Hashemi et al., 2010). Shorter T_2 was expected with the increase in the HMP concentration due to the intense interactions between the water molecules and hydrophilic parts of the HMP macromolecules (Mariette, 2009). T_2 of SFO (S_7) was measured as 140 ms, which was much shorter compared to T_2 of bulk water which could be described as several seconds (Kirtil & Oztop, 2016). Therefore, sharp T_2 decrease of the samples due to SFO addition was inevitable (Table 4). Nevertheless, similar T_2 for S_3 and S_6 showed that SFO was well dispersed in S_6 at 10% (w/w) HMP. This result (S_6) suggested that T_2 lowering effect of SFO phase was overwhelmed by efficient contribution of the oil droplets in the continuous phase (Kirtil & Oztop, 2016). Probably, presence of HMP at high concentration (10%, w/w) in continuous phase of the emulsion created a sufficient thickness of aqueous layer around the individual oil droplets (Mariette, 2009). Therefore, HMP containing continuous phase predominated the transverse relaxation. Particle size and rheology results also supported the T_2 findings. Lower span values of S_6 samples, substantial increase in the viscosity and shear-thinning behavior of S_6 formulations with respect to S_5 were also attributed to better SFO dispersion in the emulsions at 10% (w/w) HMP concentration (Huang et al., 2001). Compensation of T_2 lowering effect of SFO at 10% (w/w) HMP may have also indicated that HMP has demonstrated some surface activity. Slight hydrophobic character of HMP which was mainly originated from the high number of methyl esterified carboxyl groups could be responsible for this activity (Dickinson, 2003). Methyl esterified carboxyl groups of HMP have affinity for oil droplet surfaces and can weakly adsorb onto the oil droplet surfaces (Huang et al., 2001). Galacturonic acids and nonesterified carboxyl groups of HMP has affinity for water due to their hydrophilic characters (Mohnen, 2008). After applying high shears, rigid galacturonic acid backbone of HMP may migrate slowly to oil–water interface and contribute to the layer formation around the droplets (Garti & Reichman, 1993). These properties of HMP may have also contributed to the stabilization of the S_6 emulsions.

Table 4 also shows the effect of SFW addition to HMP solutions. When 5% (w/w) SFW was added to only HMP containing (S_8 to S_{10}) solutions, T_2 values decreased significantly (S_1 to S_3; $P < 0.05$). Shorter T_2 was due to the solidified form of SFW in the emulsions and low interaction of SFW with bulk water (Marigheto et al., 2007). Very low T_2 of pure SFW (S_{15} around 37 ms) also verified the T_2 results of wax containing emulsion. Effect of SFW addition on T_2 was also compared in Table 5 prepared to compare the T_2 values of HMP–SFO and HMP–SFO–SFW emulsions. T_2 of HMP and SFO containing samples (S_{11} to S_{13}) decreased after the addition of 5% (w/w) SFW (S_4 to S_6; $P < 0.05$). Despite the aforementioned characteristics of SFW, HMP was also able to disperse wax particles since S_6 and S_{13} attained similar T_2 values as in the case of SFO containing samples ($P > 0.05$; Table 5). Particle size measurements were also consistent with this result. As previously explained, 10% (w/w) HMP concentration reduced the mean particle size of only HMP–SFW containing emulsions ($P < 0.05$). Minor amphiphilic character of SFW and slight hydrophobicity of HMP may have contributed to the SFW dispersion in the samples in addition to the increased emulsion viscosity, which was the main factor for SFW dispersion (Baümler et al., 2013; Panchev, Nikolova, & Pashova, 2009).

3.3.2 Transverse relaxation spectrum analysis. Detailed analysis of transverse relaxations was performed by inverse Laplace transformation to obtain one dimensional relaxation distribution for each decay. Relaxation spectra of the samples represent distinct proton populations contributing to the magnetization decay (Mariette, 2009). Table 6 shows the relative peak time and area values of the samples (S_1 to S_6). These emulsions revealed three peaks with

Table 6–Transverse relaxation spectrum analysis of the emulsions.[a]

Sample	Peak 1 (ms)	Area 1 (%)	Peak 2 (ms)	Area 2 (%)	Peak 3 (ms)	Area 3 (%)
S_1	6.95 ± 0.21^{ab}	7.66 ± 1.07^{a}	18.50 ± 0.71^{c}	4.14 ± 0.16^{b}	315.00 ± 7.07^{a}	88.20 ± 0.93^{a}
S_2	7.50 ± 0.57^{ab}	9.96 ± 1.07^{a}	21.00 ± 0.05^{bc}	3.17 ± 0.01^{b}	200.00 ± 0.08^{c}	86.87 ± 1.09^{a}
S_3	6.50 ± 0.42^{ab}	11.17 ± 1.63^{a}	21.00 ± 2.83^{bc}	3.03 ± 0.44^{b}	120.00 ± 0.07^{d}	85.81 ± 2.08^{a}
S_4	9.35 ± 0.35^{a}	7.73 ± 0.46^{a}	44.00 ± 2.83^{a}	7.02 ± 0.20^{a}	255.00 ± 21.21^{b}	83.32 ± 0.74^{a}
S_5	8.50 ± 0.28^{a}	7.67 ± 0.21^{a}	28.00 ± 0.09^{b}	4.66 ± 0.50^{ab}	180.00 ± 14.14^{c}	87.68 ± 0.29^{a}
S_6	4.60 ± 1.84^{b}	10.53 ± 2.91^{a}	14.50 ± 2.12^{c}	6.80 ± 1.42^{a}	110.00 ± 0.00^{d}	81.98 ± 3.35^{a}

[a]Different inline letters in each column indicate significant difference ($P < 0.05$). Errors are represented as standard deviations.

distinct peak time and area values meaning that emulsions had three distinct proton populations with varying transverse relaxation rates. First peak with the lowest relaxation time and area was attributed to the exchangeable solid signal mainly coming from the SFW particles in the emulsions (Marigheto et al., 2007). Increasing HMP concentration did not affect the peak time and area values of S_1 to S_3 in this case (Table 6). Peak 1 times of S_4 and S_5 were not affected by SFO addition and maintained similar trend with S_1 to S_3. Unlike other SFO containing emulsions, S_6 had a lower peak time at 4.6 ms ($P < 0.05$). Better emulsion characteristics at 10% (w/w) HMP reduced the average size of the SFW particles as previously shown in Figure 2. In this way, SFW particles may have attained a higher surface to volume ratio increasing the contact area between the SFW particles and water. This may have promoted a more efficient and faster energy exchange between the solid (SFW) and liquid (water) phases (Kirtil & Oztop, 2016). Namely, the energy generated due to the relaxation of the excited SFW protons was exchanged faster with the surrounding environment (Marigheto et al., 2007). Thus, peak 1 time of S_6 decreased ($P < 0.05$).

Peak 2 signal was mainly associated with the hydration layer around the SFW particles (Liu et al., 2016). More HMP addition did not change the times and areas belonging to S_1 to S_3 samples with no dispersed oil phase. However, adding 10% (w/w) SFO to the HMP–SFW emulsions suddenly increased the peak time and area values of S_4 ($P < 0.05$). T_2 of S_{14} (SFW–SFO mixture) was found as 142 ms close to T_2 of S_7 (pure SFO) indicating that transverse relaxation of SFO protons suppressed the SFW contribution in the mixture. Accordingly, at 5% (w/w) HMP, SFO formed some layer thickness around the SFW particles and predominated the relaxation process. With increasing HMP concentrations, this T_2 increasing effect of SFO for peak 2 diminished and T_2 returned to its range observed for S_1 to S_3. Main reason for this trend was the more homogenous distribution of the oil droplets within the emulsion especially at 10% (w/w) HMP (Vermeir, Balcaen, Sabatino, Dewettinck, & Van der Meeren, 2014). Higher areas of peak 2 for S_4 to S_6 with respect to S_1 to S_3 areas could be attributed to the intensity of interactions in this proton population mainly driven by HMP activity on SFO droplet surfaces (Marigheto et al., 2007). Results of peak 2 unveiled the effect of HMP concentration on SFO dispersion in the emulsions. The more homogeneous distribution of oil droplets at high HMP concentration was also in agreement with the lower span values of S_3 and S_6 suggesting a similar size distribution for the dispersed oil droplets ($P < 0.05$; Riquelme et al., 2019). Additionally, enhanced pseudoplastic behaviors, for example higher consistency and lower flow behavior index values of S_3 and S_6 also supported the more homogeneous oil droplet distribution claim after the investigation of peak 2. This is because a better o/w emulsion characteristic is associated with the increased pseudoplastic behavior (Pal, 1996).

The highest peak T_2 values and relative areas were observed for peak 3, which represented the continuous water phase mainly interacting with HMP (Table 6; Vermeir et al., 2014). T_2 decreasing effect of HMP addition was ideally observed in peak 3. Both emulsion types having SFO or not attained lower T_2's in peak 3 at higher HMP concentrations similar to mono-exponential T_2 results ($P < 0.05$). Starting from 7% (w/w) HMP, more homogeneous distribution of SFO droplets (e.g., lower span values, higher pseudoplastic character and viscosity) revealed peak times in the same range for S_2 to S_5 and S_3 to S_6 samples. This was also in agreement with the compensation of mono-exponential T_2 lowering effect of SFO with increasing HMP concentration. Peak 3 areas were by far the highest compared to previous peaks

since the interactions in this proton population were dominant in determining the overall transverse relaxations of the emulsions (Ozel, Uguz, Kilercioglu, Grunin, & Oztop, 2017).

Contrary to HMP–SFW emulsions and their SFO including correspondents, multiexponential relaxation analysis of only HMP containing solutions (S_8 to S_{10}) produced one peak which was due to the dominant hydrophilic character of HMP (Yoo et al., 2009). Polymer–water interactions predominated the relaxation process of S_8 to S_{10} in the absence of SFW or SFO. All in all, relaxation spectrum analysis of the emulsion samples showed that multiexponential transverse relaxation results of the emulsions were in correlation with the previous particle size, rheology, and mono-exponential transverse relaxation analyses.

4. CONCLUSION

Emulsions showed distinct physical characteristics depending on the HMP concentration and presence of SFO and SFW. HMP was able to disperse SFW and SFO in the emulsions mainly by modifying the viscosity of the continuous phase. At 10% (w/w) concentration, HMP was more effective in forming emulsions with desired properties since particle span values decreased whereas viscosity and pseudoplastic character of the emulsions increased ($P < 0.05$). Mono-exponential T_2 relaxations and decomposition of the relaxation spectra provided detailed information regarding physico-chemical interactions taking place within the emulsions. Mono and multiexponential transverse relaxation results were in correlation with the particle size and rheology results. T_2 decreasing effect of SFO was compensated at 10% (w/w) HMP concentration which was attributed to better dispersion of SFO in the emulsions. Results indicated that SFW which is an essential material for the formation of edible films with reduced water permeability characteristics, could be integrated to film forming emulsions to some extent. Finally, this study showed that NMR relaxometry could be used as a nondestructive tool to analyze complex emulsion systems. Transverse relaxation parameters could be applied for the analysis of new HMP–SFW formulation protocols that could later be utilized to produce HMP–SFW based products such as edible films and coatings.

ACKNOWLEDGMENTS

COST Action (CA15209) is acknowledged due to the valuable discussions about the findings in Meeting's WG meetings.

AUTHOR CONTRIBUTIONS

The study is the MSc study of Ms. Sinem Akkaya. Mr. Ozel helped on the NMR results and organized the manuscript. Dr. Oztop, Dr. Gogus, and Dr. Yanık were the graduate advisors of Ms. Akkaya during the thesis work.

CONFLICTS OF INTEREST

Authors declare no conflict of interest for the study.

REFERENCES

Aguirre-Joya, J. A., Cerqueira, M. A., Ventura-Sobrevilla, J., Aguilar-Gonzalez, M. A., Carbó-Argibay, E., Castro, L. P., & Aguilar, C. N. (2019). Candelilla Wax-Based Coatings and Films: Functional and Physicochemical Characterization. *Food and Bioprocess Technology*, *12*(10), 1787–1797. https://doi.org/10.1007/s11947-019-02339-2

Akhtar, M., Dickinson, E., Mazoyer, J., & Langendorff, V. (2002). Emulsion stabilizing properties of depolymerized pectin. *Food Hydrocolloids*, *16*(3), 249–256. https://doi.org/10.1016/S0268-005x(01)00095-9

Asumadu-Mensah, A., Smith, K. W., & Ribeiro, H. S. (2013). Solid lipid dispersions: Potential delivery system for functional ingredients in foods. *Journal of Food Science*, *78*(7), 1000–1008. https://doi.org/10.1111/1750-3841.12162

Barnes, H. A. (1994). Rheology of emulsions - a review. *Colloids and Surfaces A: Physicochemical and Engineering Aspects*, *91*, 89–95. https://doi.org/10.1016/0927-7757(93)02719-U

Baümler, E. R., Carelli, A. A., & Martini, S. (2013). Physical properties of aqueous solutions of pectin containing sunflower wax. *JAOCS, Journal of the American Oil Chemists' Society*, *90*(6), 791–802. https://doi.org/10.1007/s11746-013-2235-y

Chalapud, M. C., Baümler, E. R., & Carelli, A. A. (2018). Emulsions of sunflower wax in pectin aqueous solutions: Physical characterization and stability. *Food Research International*, *108*(March), 216–225. https://doi.org/10.1016/j.foodres.2018.03.053

Chalapud, M. C., Baümler, E. R., & Carelli, A. A. (2020). Edible films based on aqueous emulsions of low-methoxyl pectin with recovered and purified sunflower waxes. *Journal of the Science of Food and Agriculture*, *100*(6), 2675–2687. https://doi.org/10.1002/jsfa.10298

Chanamai, R., & McClements, D. J. (2002). Comparison of Gum Arabic, Modified Starch, and Whey Protein Isolate as Emulsifiers : Influence of pH, CaCl2 and Temperature. *Journal of Food Chemistry and Toxicology*, *67*(1), 120–125. https://doi.org/10.1111/j.1365-2621.2002.tb11370.x

Derkach, S. R. (2009). Rheology of Emulsions. *Advances in Colloid and Interface Science*, *151*, 1–23. https://doi.org/10.1016/j.cis.2009.07.001

Dickinson, E. (2003). Hydrocolloids at interfaces and the influence on the properties of dispersed systems. *Food Hydrocolloids*, *17*, 25–39. www.elsevier.com/locate/foodhyd

Dickinson, E. (2009). Hydrocolloids as emulsifiers and emulsion stabilizers. *Food Hydrocolloids*, *23*(6), 1473–1482. https://doi.org/10.1016/j.foodhyd.2008.08.005

Galus, S., & Kadzińska, J. (2015). Food applications of emulsion-based edible films and coatings. *Trends in Food Science and Technology*, *45*(2), 273–283. https://doi.org/10.1016/j.tifs.2015.07.011

Garti, N., & Reichman, D. (1993). Hydrocolloids as Food Emulsifiers and Stabilizers. *Food Structure*, *12*(4), 411–426. http://digitalcommons.usu.edu/foodmicrostructurehttp://digitalcommons.usu.edu/foodmicrostructure/vol12/iss4/3

Guner, S., & Oztop, M. H. (2017). Food grade liposome systems: Effect of solvent, homogenization types and storage conditions on oxidative and physical stability. *Colloids and Surfaces A: Physicochemical and Engineering Aspects*, *513*, 468–478. https://doi.org/10.1016/j.colsurfa.2016.11.022

Guzey, D., & McClements, D. J. (2006). Formation, stability and properties of multilayer emulsions for application in the food industry. *Advances in Colloid and Interface Science*, *128–130*(2006), 227–248. https://doi.org/10.1016/j.cis.2006.11.021

Hashemi, R. H., Bradley, W. G., & Lisanti, C. J. (2010). *MRI: The basics* (3rd ed.). Baltimore: Lippincott Williams and Wilkins.

Huang, X., Kakuda, Y., & Cui, W. (2001). Hydrocolloids in emulsions: Particle size distribution and interfacial activity. *Food Hydrocolloids*, *15*(4–6), 533–542. https://doi.org/10.1016/S0268-005X(01)00091-1

Jafari, S. M., Assadpoor, E., He, Y., & Bhandari, B. (2008). Re-coalescence of emulsion droplets during high-energy emulsification. *Food Hydrocolloids*, *22*(7), 1191–1202. https://doi.org/10.1016/j.foodhyd.2007.09.006

Karbstein, H., & Schubert, H. (1995). Developments in the continuous mechanical production of oil-in-water macro-emulsions. *Chemical Engineering and Processing*, *34*(3), 205–211. https://doi.org/10.1016/0255-2701(94)04005-2

Kim, H. S., & Mason, T. G. (2017). Advances and challenges in the rheology of concentrated emulsions and nanoemulsions. *Advances in Colloid and Interface Science*, *247*(July), 397–412. https://doi.org/10.1016/j.cis.2017.07.002

Kirtil, E., & Oztop, M. H. (2016). 1H Nuclear Magnetic Resonance Relaxometry and Magnetic Resonance Imaging and Applications in Food Science and Processing. *Food Engineering Reviews*, *8*(1), 1–22. https://doi.org/10.1007/s12393-015-9118-y

Kowalczyk, D., Zięba, E., Skrzypek, T., & Baraniak, B. (2017). Effect of carboxymethyl cellulose/candelilla wax coating containing ascorbic acid on quality of walnut (Juglans regia L.) kernels. *International Journal of Food Science and Technology*, *52*(6), 1425–1431. https://doi.org/10.1111/ijfs.13420

Lee, R. F. (1999). Agents which promote and stabilize water-in-oil emulsions. *Spill Science and Technology Bulletin*, *5*(2), 117–126. https://doi.org/10.1016/S1353-2561(98)00028-0

Leroux, J., Langendorff, V., Schick, G., Vaishnav, V., & Mazoyer, J. (2003). Emulsion stabilizing properties of pectin. *Food Hydrocolloids*, *17*(4), 455–462. https://doi.org/10.1016/S0268-005X(03)00027-4

Linke, C., Guthausen, G., Flöter, E., & Drusch, S. (2018). Solid Fat Content Determination of Dispersed Lipids by Time-Domain NMR. *European Journal of Lipid Science and Technology*, *120*(4), 1–8. https://doi.org/10.1002/ejlt.201700132

Liu, Y., Gajewicz, A. M., Rodin, V., Soer, W. J., Scheerder, J., Satgurunathan, G., … Keddie, J. L. (2016). Explanations for water whitening in secondary dispersion and emulsion polymer films. *Journal of Polymer Science, Part B: Polymer Physics*, *54*(16), 1658–1674. https://doi.org/10.1002/polb.24070

Mariette, F. (2009). Investigations of food colloids by NMR and MRI. *Current Opinion in Colloid and Interface Science*, *14*(3), 203–211. https://doi.org/10.1016/j.cocis.2008.10.006

Marigheto, N., Venturi, L., Hibberd, D., Wright, K. M., Ferrante, G., & Hills, B. P. (2007). Methods for peak assignment in low-resolution multidimensional NMR cross-correlation relaxometry. *Journal of Magnetic Resonance*, *187*(2), 327–342. https://doi.org/10.1016/j.jmr.2007.04.016

McClements, D. J. (2015). *Food emulsions: Principles, practices and techniques* (3rd ed.). Boca Raton: CRC Press.

Mohnen, D. (2008). Pectin structure and biosynthesis. *Current Opinion in Plant Biology*, *11*(3), 266–277. https://doi.org/10.1016/j.pbi.2008.03.006

Moreau, L., Kim, H.-J., Decker, E. A., & McClements, D. J. (2003). Production and characterization of oil-in-water emulsions containing droplets stabilized by beta-lactoglobulin-pectin membranes. *Journal of Agricultural and Food Chemistry*, *51*, 6612–6617. https://doi.org/10.1021/jf034332+

Muhiddinov, Z., Khalikov, D., Speaker, T., & Fassihi, R. (2004). Development and characterization of different low methoxy pectin microcapsules by an emulsion-interface reaction technique. *Journal of Microencapsulation*, *21*(7), 729–741. https://doi.org/10.1080/02652040400008507

Nakauma, M., Funami, T., Noda, S., Ishihara, S., Al-Assaf, S., Nishinari, K., & Phillips, G. O. (2008). Comparison of sugar beet pectin, soybean soluble polysaccharide, and gum arabic as food emulsifiers. 1. Effect of concentration, pH, and salts on the emulsifying properties. *Food Hydrocolloids*, *22*(7), 1254–1267. https://doi.org/10.1016/j.foodhyd.2007.09.004

Okuro, P. K., Gomes, A., Costa, A. L. R., Adame, M. A., & Cunha, R. L. (2019). Formation and stability of W/O-high internal phase emulsions (HIPEs) and derived O/W emulsions stabilized by PGPR and lecithin. *Food Research International*, *122*(April), 252–262. https://doi.org/10.1016/j.foodres.2019.04.028

Ozel, B., Uguz, S. S., Kilercioglu, M., Grunin, L., & Oztop, M. H. (2017). Effect of different polysaccharides on swelling of composite whey protein hydrogels: A low field (LF) NMR

relaxometry study. *Journal of Food Process Engineering*, *40*(3), 1–9. https://doi.org/10.1111/jfpe.12465

Oztop, M. H., Rosenberg, M., Rosenberg, Y., McCarthy, K. L., & McCarthy, M. J. (2010). Magnetic resonance imaging (MRI) and relaxation spectrum analysis as methods to investigate swelling in whey protein gels. *Journal of Food Science*, *75*(8), 508–515. https://doi.org/10.1111/j.1750-3841.2010.01788.x

Pal, R. (1996). Effect of Droplet Size on the Rheology of Emulsions. *AIChE Journal*, *42*(11), 3181–3190. https://doi.org/10.1002/aic.690421119

Panchev, I., Nikolova, K. R., & Pashova, S. (2009). Physical characteristics of wax-containing pectin aqueous solutions. *Journal of Optoelectronics and Advanced Materials*, *11*(9), 1214–1217.

Pocan, P., Ilhan, E., & Oztop, M. H. (2019). Characterization of Emulsion Stabilization Properties of Gum Tragacanth, Xanthan Gum and Sucrose Monopalmitate: A Comparative Study. *Journal of Food Science*, *84*(5), 1087–1093. https://doi.org/10.1111/1750-3841.14602

Riquelme, N., Zúñiga, R. N., & Arancibia, C. (2019). Physical stability of nanoemulsions with emulsifier mixtures: Replacement of tween 80 with quillaja saponin. *LWT - Food Science and Technology*, *111*(February), 760–766. https://doi.org/10.1016/j.lwt.2019.05.067

Sahin, S., & Sumnu, S. G. (2006). Rheological properties of foods. In D. R. Heldman (Ed.). *Physical properties of foods*. New York: Springer Science.

Tabilo-Munizaga, G., & Barbosa-Cánovas, G. V. (2005). Rheology for the food industry. *Journal of Food Engineering*, *67*(1–2), 147–156. https://doi.org/10.1016/j.jfoodeng.2004.05.062

Taherian, A. R., Fustier, P., Britten, M., & Ramaswamy, H. S. (2008). Rheology and stability of beverage emulsions in the presence and absence of weighting agents: A review. *Food Biophysics*, *3*(3), 279–286. https://doi.org/10.1007/s11483-008-9093-4

Thakur, B. R., Singh, R. K., & Handa, A. K. (1997). Chemistry and Uses of Pectin - A Review. *Critical Reviews in Food Science and Nutrition*, *37*(1), 47–73. https://doi.org/10.1080/10408399709527767

Thombre, N. A., & Gide, P. S. (2013). Rheological characterization of galactomannans extracted from seeds of Caesalpinia pulcherrima. *Carbohydrate Polymers*, *94*(1), 547–554. https://doi.org/10.1016/j.carbpol.2013.01.051

Ushikubo, F. Y., & Cunha, R. L. (2014). Stability mechanisms of liquid water-in-oil emulsions. *Food Hydrocolloids*, *34*, 145–153. https://doi.org/10.1016/j.foodhyd.2012.11.016

Vargas, M., Pastor, C., Chiralt, A., McClements, D. J., & González-Martínez, C. (2008). Recent advances in edible coatings for fresh and minimally processed fruits. *Critical Reviews in Food Science and Nutrition*, *48*(6), 496–511. https://doi.org/10.1080/10408390701537344

Vélez-Erazo, E. M., Bosqui, K., Rabelo, R. S., Kurozawa, L. E., & Hubinger, M. D. (2020). High internal phase emulsions (HIPE) using pea protein and different polysaccharides as stabilizers. *Food Hydrocolloids*, *105*, October 2019). https://doi.org/10.1016/j.foodhyd.2020.105775

Vermeir, L., Balcaen, M., Sabatino, P., Dewettinck, K., & Van der Meeren, P. (2014). Influence of molecular exchange on the enclosed water volume fraction of W/O/W double emulsions as determined by low-resolution NMR diffusometry and T2-relaxometry. *Colloids and Surfaces A: Physicochemical and Engineering Aspects*, *456*(1), 129–138. https://doi.org/10.1016/j.colsurfa.2014.05.022

Williams, P. D., Oztop, M. H., Mccarthy, M. J., Mccarthy, K. L., & Lo, Y. M. (2011). Characterization of water distribution in xanthan-curdlan hydrogel complex using magnetic resonance imaging, nuclear magnetic resonance relaxometry, rheology, and scanning electron microscopy. *Journal of Food Science*, *76*(6), 472–478. https://doi.org/10.1111/j.1750-3841.2011.02227.x

Xiong, W., Ren, C., Tian, M., Yang, X., Li, J., & Li, B. (2018). Emulsion stability and dilatational viscoelasticity of ovalbumin/chitosan complexes at the oil-in-water interface. *Food Chemistry*, *252*(January), 181–188. https://doi.org/10.1016/j.foodchem.2018.01.067

Yoo, Y. H., Lee, S., Kim, Y., Kim, K. O., Kim, Y. S., & Yoo, S. H. (2009). Functional characterization of the gels prepared with pectin methylesterase (PME)-treated pectins. *International Journal of Biological Macromolecules*, *45*(3), 226–230. https://doi.org/10.1016/j.ijbiomac.2009.05.005

Zhang, Y., Simpson, B. K., & Dumont, M. J. (2018). Effect of beeswax and carnauba wax addition on properties of gelatin films: A comparative study. *Food Bioscience*, *26*(October), 88–95. https://doi.org/10.1016/j.fbio.2018.09.011